

Received 23 October 2023, accepted 10 November 2023, date of publication 13 November 2023,  
date of current version 17 November 2023.

Digital Object Identifier 10.1109/ACCESS.2023.3332541

## RESEARCH ARTICLE

# IVNet: Transfer Learning Based Diagnosis of Breast Cancer Grading Using Histopathological Images of Infected Cells

SAMEEN AZIZ<sup>1</sup>, KASHIF MUNIR<sup>1</sup>, ALI RAZA<sup>2</sup>, MUBARAK S. ALMUTAIRI<sup>3</sup>,  
AND SHOAB NAWAZ<sup>4</sup>

<sup>1</sup>Institute of Information Technology, Khwaja Fareed University of Engineering and Information Technology, Rahim Yar Khan 64200, Pakistan

<sup>2</sup>Institute of Computer Science, Khwaja Fareed University of Engineering and Information Technology, Rahim Yar Khan 64200, Pakistan

<sup>3</sup>College of Computer Science and Engineering, University of Hafr Al Batin, Hafr Al Batin 31991, Saudi Arabia

<sup>4</sup>University of South Asia, Lahore 54792, Pakistan

Corresponding author: Kashif Munir (kashif.munir@kfueit.edu.pk)

This work was supported by the University of Hafr Al Batin, Saudi Arabia.

**ABSTRACT** Breast cancer constitutes a significant global health concern that impacts millions of women across the world. The diagnosis of breast cancer involves categorizing grades based on the histopathological characteristics of tumor cells. While histopathological assessment remains the established benchmark for breast cancer diagnosis, it is hampered by time-consuming procedures, subjectivity, and susceptibility to human errors. This study introduces a novel approach called ImageNet-VGG16 (IVNet) for the real-time diagnosis of breast cancer within a hospital environment. The research experiments are conducted using a benchmark dataset known as Jimma University Medical Center (JUMC) breast cancer grading. Advanced image processing techniques are applied to preprocess the data, enhancing performance. This preprocessing involves the utilization of Holistically Nested Edge Detection (HED) and Contrast Limited Adaptive Histogram Equalization (CLAHE) for transformation and stain normalization. We employ advanced neural network-based transfer learning techniques to analyze the preprocessed histopathological images and identify affected cells. Various pre-trained models are utilized, including convolutional neural networks (CNN) such as VGG16, ResNet50, InceptionNetv3, ImageNet, MobileNetv3, and EfficientNetV3, in a comparative framework. The principal objective of this research is the accurate classification of breast cancer images into Grade-1, Grade-2 and Grade-3. Through extensive experimental research, we achieved a commendable 97% correct classification rate by utilizing a hybrid of VGG16 and ImageNet as the proposed feature engineering method, IVNet. We also validate our proposed approach performance using other state-of-the-art study data and statistical t-test analysis. Furthermore, we develop a user-friendly Graphical User Interface (GUI) that facilitates real-time cell tracking in histopathological images. Our real-time diagnosing application offers valuable insights for treatment planning and assists medical professionals in making prognoses. Moreover, our approach can serve as a reliable decision support system for pathologists and clinicians, particularly in settings constrained by limited resources and restricted access to expertise and equipment.

**INDEX TERMS** Breast cancer, cancer grading, image processing, deep learning, machine learning, transfer learning, biomedical engineering.

## I. INTRODUCTION

Breast cancer arises when abnormal breast cells multiply uncontrollably [1]. It has various categories, subtypes, and

The associate editor coordinating the review of this manuscript and approving it for publication was Ines Domingues<sup>1</sup>.

grades based on cell size, shape, and behavior. Subtypes indicate the origin of breast cancer, such as milk ducts, lobules, or connective tissue [2]. Cancer cells determine whether breast cancer is tubular, mucinous, or papillary. The grade of breast cancer depends on how quickly cancer cells proliferate and spread. The traditional breast cancer

grading system assigns a grade of 1 to well-differentiated, slow-progressing cancer and 3 to poorly differentiated, fast-progressing cancer. Staging breast cancer is another important aspect, as it helps determine the extent of the cancer's spread. Breast cancer severity is classified by tumor size, lymph node involvement, and distant metastases. Stage 0 corresponds to non-invasive breast cancer, while stage 4 indicates metastatic disease [3]. Identifying the subtype, grade, and stage of breast cancer is crucial for doctors to develop appropriate patient treatment plans.

The breast biopsy samples are examined under a microscope during classical diagnosis to detect potential abnormalities [4], [5]. Breast biopsies serve to identify both cancerous and non-cancerous conditions. Various methods for breast biopsy exist, such as fine needle aspiration, core needle biopsy, vacuum-assisted biopsy, and surgical biopsy [6]. The choice of procedure depends on factors such as the size, location, and appearance of the breast abnormality. A local anaesthetic is administered during the biopsy to numb the breast area while keeping the patient conscious. Temporary bruising, swelling, and bleeding at the biopsy site are common occurrences [7]. The CDC recommends regular breast checks as a means to diagnose breast cancer. During these checks, healthcare professionals examine the breasts and the armpit lymph nodes for any signs of tumors or abnormalities. If unusual findings arise, the doctor might suggest further testing, including mammograms, to identify subtle yet significant breast tissue changes. Ultrasound imaging, employing high-frequency sound waves, produces visual representations of the breast [8]. Additionally, breast MRI, utilizing magnets and radio waves, generates high-resolution images of the breast and the adjacent tissue.

Biopsies involve the removal of breast tissue or fluid for microscopic inspection and diagnosis [9]. Different biopsies are available, including core, fine-needle, and open biopsies. A confirmed diagnosis of breast cancer relies on biopsy results. The biopsy sample's cell type, grade, and receptor status determine the appropriate cancer treatment [10]. Following a breast cancer diagnosis, additional tests may be conducted to determine the extent of the illness and whether it has spread. Treatment decisions are influenced by disease staging. The diagnosis of the most common type of breast cancer, Invasive Ductal Carcinoma (IDC), involves the use of imaging, physical examinations, and tissue pathology [11]. Methods such as mammography, ultrasonography, and MRI are employed for diagnosing IDC breast cancer. Clinical examinations conducted by medical professionals can detect breast tumors, changes in size, and other symptoms associated with breast cancer.

During classical diagnosis, a biopsy is conducted if imaging or clinical examination reveals an anomaly [12]. A surgical core needle and fine-needle aspiration biopsies are common examples. Once the sample is sent to a lab, a pathologist will analyze it. The pathologist examines the biopsy sample for the presence of cancer cells and their distinguishing features. The pathologist must identify cancer

cells beyond the breast ducts in surrounding tissues to diagnose IDC [13]. Following an IDC diagnosis, additional tests may be performed to determine the cancer's stage and to screen for potential metastasis. These examinations may encompass X-rays, CT scans, and PET scans. Breast cancer cells are graded under microscopic analysis to estimate their aggressiveness and potential for metastasis. The Nottingham grading system (Elstone-Ellis) is the gold standard for classifying breast cancer [14]. It evaluates three key traits of cancer cells: their resemblance to breast cells when forming tubules. Low-grade, high-tubule cancers are generally less aggressive.

Nuclear pleomorphism, which involves nucleus size, shape, and staining variation, is prevalent in malignant cells [15]. High-grade tumors exhibit more significant nuclear abnormalities, indicating a higher level of aggression. The mitotic index of cancerous tissue measures the rate of cell divisions. A higher mitotic count suggests faster cell division and proliferation, indicating a higher grade. Determining the grade involves assessing tubule development, nuclear pleomorphism, and mitotic activity [16]. The presence of these features is combined [17] to assign a grade. Higher grades imply a more aggressive cancer with an elevated risk of metastasis. It is important to remember that when evaluating breast cancer, factors such as tumor size, lymph node involvement, and molecular traits are equally significant alongside the cancer grade. Machine learning techniques, particularly transfer learning, have demonstrated potential in diagnosing IDC breast cancer [18]. Transfer learning involves leveraging pre-trained models from large datasets to improve the performance of models on smaller datasets. This approach holds promise for accurate IDC breast cancer diagnosis through transfer learning.

In this research, we have proposed an innovative IVNet method for diagnosing breast cancer grading. We utilized a cutting-edge dataset JUMC Breast Cancer Grading, for building applied models. Our proposed method harnesses deep learning techniques to analyze histopathological images and identify affected cells with high-performance scores compared to state-of-the-art studies [19]. We employed transfer learning approaches, utilizing pre-trained models and neural network architectures. The main objective of this research is to precisely classify breast cancer images into Grade01, Grade02, and Grade03 using an efficient transfer learning neural network.

The primary research contributions of our proposed study for the diagnosis of breast cancer are as follows:

- We have preprocessed the image dataset using the HED and CLAHE approaches for transformation and stain normalization. Transformation techniques are employed to enhance the results of breast image classification.
- A novel IVNet Method is presented for a smart feature engineering mechanism from histopathological images of infected cells, which helps improve diagnosis performance. We also validate our proposed approach

performance using other state-of-the-art study data and statistical t-test analysis.

- We have evaluated the performance using various pre-trained neural networks, including CNN, VGG16, ResNet50, InceptionNetv3, MobileNetv3, and EfficientNetV3.
- We have created a user-friendly GUI designed for real-time cell tracking within histopathological images. This real-time tracking application provides valuable insights for treatment planning and assists medical professionals in making prognostic assessments.
- We have conducted a thorough review of the current body of literature and research studies that delve into diverse methodologies and techniques to grade breast cancer through the analysis of histopathological images precisely.

The subsequent sections of this manuscript are structured as follows: Section II presents a comprehensive analysis of approaches employed in prior studies. In Section III, we detail the proposed methodology workflow analysis. The performance scores of the applied methods are comparatively evaluated in Section IV. Our proposed research findings are summarized in Section V.

## II. LITERATURE ANALYSIS

This section comprehensively reviews the existing literature and research studies investigating various methodologies and techniques for accurately grading breast cancer using histopathological images [20]. We aim to identify the strengths, limitations, and gaps in the current knowledge landscape by synthesizing and analyzing prior research. We critically evaluate the performance metrics of the methodologies, the datasets employed, and their overall effectiveness in distinguishing between distinct cancer grades.

DeepGrade, a deep learning-based method for histologically grading breast malignancies based on digitized hematoxylin and eosin (HE)-stained WSIs, is proposed in this study [21]. The research states that breast cancer histological grade, which considers both morphology and proliferation, has unique predictive value and is widely used in clinical decision-making [22]. It offers Deep Grade, a deep learning-based method for histologically grading breast malignancies based on digitized hematoxylin and eosin (HE)-stained WSIs, emphasizing enhancing prognostic classification of NHG 2 tumors. The model classified NHG 1 and NHG 3 morphological patterns and restratified NHG 2 tumors using the learned patterns. The model-based categorization of NHG 2 tumor patients is prognostic and adds clinically useful information to histological grading. Deep Grade was used to grade breast tumors histologically using digitized hematoxylin and eosin (HE)-stained WSIs. Patient outcome data from independent internal and external tests verified the suggested model. If a subgroup's minimum value is less than 5, Fisher's exact test or chi-square test was used to compare categorical variable distributions. The t-test

examined mean age differences. The ManneWhitney U test compared Ki67 scores. A two-sided P value  $<0.05$  was statistically significant.

This study [23] develops and evaluates breast cancer histologic grading deep learning models. The article used digital hematoxylin and eosin-stained slides of invasive breast cancer from a tertiary teaching hospital, a medical laboratory, and TCGA. Qualified pathologists assessed all whole-slide images (WSIs) for slide-level inclusion and quality assurance. TTH, MLAB, and TCGA datasets were used to construct and test deep learning models [31], [32]. Slides with a pathologist majority examined the component models to achieve performance assessment reference dependability. The paper showed that deep learning can grade breast cancer and pathologists. The research includes patch- and slide-level model assessment measures. The research only included digital hematoxylin and eosin-stained slides of invasive breast cancer from formalin-fixed paraffin-embedded resection tissues.

In this study [24], a deep learning-based approach for automated breast cancer grading on whole-slide photos. The approach classifies tumors into two categories, low/intermediate and high grade, and discovers a pattern in survival for each. All of the young (40) Dutch women who were diagnosed with invasive ductal carcinoma in situ (invasive ductal carcinoma in situ) without (lymph node) metastases between 1989 and 2000 were included in the PARADIGM study. These women had no history of other malignancies and had not received adjuvant systemic treatment per current guidelines. Whole-slide pictures from 706 patients with invasive breast cancer and their accompanying tumor grade (low/intermediate vs. high) and its components nuclear grade, tubule formation, and mitotic rate were used to build and test a deep learning-based model. The model's accuracy was measured against ground-truth annotations from experienced pathologists in a test set of 686 cases using Cohen's kappa. With a Cohen's Kappa of 0.59 (80% accuracy), the deep learning system was able to discern between low/intermediate and high tumor grades in comparison to human pathologists.

Consistent reporting and grading of invasive breast cancer pathology data across countries is the subject of discussion in this research [25]. The objective is to establish a global standard for reporting and assessing pathology data concerning invasive breast cancer. The new worldwide dataset for pathology reporting, developed by the International Consortium for Cancer Reporting (ICCR), encompasses breast cancer resection specimens featuring invasive cancer and ductal carcinoma in situ (DCIS). Leading breast pathologists, a surgeon, and an oncologist from around the globe collaborated to compile this information. The dataset comprises both mandatory and discretionary pieces of information. The subsequent phase involves an international round of public feedback, following which the synoptic reporting guide will be approved and made available on the ICCR website, accessible to the public at no charge.

**TABLE 1. The literature summary and research gap analysis.**

Ref	Paradigm	Dataset	Findings	Limitation Gap
[21]	Deep learning-based approach, DeepGrade	WSIs stained, 1567 patients for model optimization and validation and 1262 patients for testing	Improves risk categorization and offers independent prognostic information for Nottingham histological grade 2 breast cancer patients.	Just improve the images digital whole-slide histopathology images (WSIs) not available in all clinical
[23]	Deep learning models to perform histologic scoring	Tertiary teaching hospital (TTH), a medical laboratory (MLAB), and The Cancer Genome Atlas (TCGA), whole-slide images (WSIs)	Developed deep learning models to perform histologic scoring of all three components of the Nottingham Grading System (NGS) using digitized hematoxylin and eosin-stained slides containing invasive breast carcinoma	Only included digitized hematoxylin and eosin-stained slides containing invasive breast carcinoma
[24]	Deep learning-based breast cancer grading model was developed using whole-slide images	Subject clinical data, whole slide images, and pathological reviews, this dataset is not publicly available	Cancer grading model developed in this study can distinguish between low/intermediate and high-grade tumors with a Cohen's Kappa of 0.59 (80% accuracy) compared to expert pathologists	Only included young (<40 years) invasive breast cancer patients
[25]	Does not describe a specific research method as it is an overview of the (ICCR) and provide a standardized approach to reporting and grading.	Invasive cancer and ductal carcinoma in situ (DCIS) of the breast.	Promote high-quality, standardized pathology reporting, development of the dataset, and the process involved in its creation.	Challenges in implementing the dataset in different regions or countries due to differences in healthcare systems, resources, and practices.
[26]	Nuclei-aware network method for grading of breast cancer in HE stained pathological images	Grading of breast Invasive Ductal Carcinoma (IDC)	Nuclei-aware network method for grading of breast cancer in HE stained pathological images	Valuated on a specific dataset and further validation on larger datasets
[27]	Automated Nottingham Grading System (NGS) framework using deep learning	Cases of consecutive invasive breast carcinoma from a single year (2016) in the pathology files	Concordance in breast carcinoma grading between AI and pathologists using digital WSI was comparable	Study was conducted on a relatively small cohort of 137 invasive breast carcinomas from a single year (2016) at a single institution.
[28]	Two full-face tumor sections were cut from 97 cases, stained with H&E only, and the other was stained with PHH3 counterstained with H&E.	A cohort of primary invasive breast cancer patients as the dataset	The PHH3 counterstained with H&E technique	Small sample size of 97 cases
[29]	Deep-learning model trained on a convolutional neural network-based algorithm (CNN-bA) to evaluate breast ductal carcinoma grading.	The 100 cases of ductal adenocarcinoma of the breast (DAC-NOS) that were randomly selected from the TCGA-BRCA WSI dataset	Trained a deep-learning model using a convolutional neural network-based algorithm (CNN-bA) on 100 whole slide images (WSIs) of ductal adenocarcinoma enhance the accuracy and reproducibility of breast cancer grading	ROIs evaluated by the AI model were not identical to the ROIs evaluated by the pathologists
[30]	Whole slide images (WSI) and artificial intelligence (AI) to investigate whether mitoses counting in breast cancer (BC) compares better to light microscopy (LM) when assisted by AI	Dataset of fifty breast cancer patients with paired core biopsies and resections	Mitoses counting on digital whole slide images (WSI) can be done well with the help of artificial intelligence (AI) and that the presented AI algorithm for pathologist supervised use in daily practice is validated.	Small sample size of 50 breast cancer patients, which may limit the generalizability of the findings.

This paper presents an overview of the International ICCR Software Application, designed to standardize the reporting and grading of pathology data pertaining to invasive breast cancer internationally.

In the context of detecting breast cancer in HE-stained pathological images, the authors of this research propose the utilization of a nuclei-aware network [26]. This network employs an attention-based approach to learn feature representations that are both fine-grained and intricately connected to nuclei, specifically for rating IDC. The mechanism resembles an attention process in end-to-end learning. The experimental findings validate the suggested technique's superiority over the current gold standard. The article focuses on determining breast cancer grades using HE-stained pathology images. The experimental results clearly illustrate

that the proposed nuclei-aware network technique attains higher accuracy rates in classifying breast cancer grades compared to state-of-the-art methods. Receiver Operating Characteristic (ROC) analysis indicates an average Area Under the Curve (AUC) of 0.93, with corresponding values of 0.94, 0.91, and 0.93.

The research [27] analyzes the agreement between AI and a group of breast pathologists from various institutions using digital whole slide imaging (WSI) to grade breast carcinomas. According to the results, AI demonstrated comparable concordance with pathologists, employing only explicable approaches. The paper employed machine learning techniques on a cohort of 143 instances, excluding 2 due to computational issues and 4 that were corrupted. A total of 137 whole slide images (WSIs) were used for

the final analysis: 46 for the training set and the remaining 91 for the testing set. A single pathologist annotated the WSIs for the invasive tumor area and the leading edge. Through deep learning, the authors automated the Nottingham Grading System (NGS). They graded 137 invasive carcinoma slides using scores for tubule formation (TF), nuclear pleomorphism (NP), and mitotic count (MC), with six pathologists and a computer algorithm providing the grades. Complete agreement was observed in 25 instances. Overall, AI exhibited an accuracy of 0.659 (compared to the designated grade in the test set), 0.758 (for TF), 0.802 (for NP), and 0.659 (for MC). When comparing the AI-generated grades to the reported grades, it achieved a 70% accuracy for grades 1 and 2 and a 52% accuracy for grade 3 breast cancer.

The findings in [28] demonstrate that H&E staining tends to assign lower grades to breast carcinomas (BCs) compared to PHH3 staining, which in turn affects staging, prognosis, and treatment decisions. Factors such as higher tumor stage, a tumor size of 2 cm, high-grade morphology, nuclear pleomorphism, reduced tubule formation, and a high Nottingham Prognostic Index (NPI) were all found to be strongly associated with positive PHH3 expression in this breast cancer research. The presence of PHH3 positivity was correlated with lower Breast Cancer-Specific Survival (BCSS) rates and shorter Distant Metastasis-Free Survival (DMFS) times. Addressing the variations in breast cancer grading observed among pathologists, this paper introduces a deep learning model based on a convolutional neural network approach (CNN-bA). The model was trained using 100 Whole Slide Images (WSIs) of Ductal Carcinoma in Situ (DAC-NOS) sourced from the TCGA-BRCA dataset, which encompasses cases of invasive breast cancer. In preparation for next-generation sequencing (NGS) analysis, a thoracic pathologist manually delineated the training dataset to annotate all tissue and cell attributes. To mitigate the limited size of the training dataset, the research employed Aiforia's image augmentation features. The developed grading AI model necessitated a total of 17 hours, 34 minutes, and 44 seconds, along with 19,000 iterations, to complete its training process.

In [29], the model's grading was generally in accordance with that of general pathologists, except for the mitotic count score, which exhibited the least concordance. According to the study, following 17.5 hours and 19,000 iterations, a deep-learning model trained using a convolutional neural network-based method (CNN-bA) demonstrated good accuracy, sensitivity, and F1 scores across several grading components. Regarding NGS components, tubule segmentation displayed the lowest accuracy (precision = 94.95, sensitivity = 94.49, F1 score = 94.73). A total of 232 patients were included in this study. No differences in survival rates were observed between those with HER2-low and HER2-zero malignancies.

This study [30] compares and contrasts the utilization of digital whole slide imaging (WSI) and light microscopy (LM) for mitosis counting in breast cancer. The research results lend support to the feasibility of mitosis counting on WSI and validate the provided AI algorithm for application in everyday

practice under the guidance of pathologists. Fifty breast cancer patients who had undergone paired core biopsies and resections were randomly selected for inclusion in this article. Mitotic count (MC) was assessed using light microscopy (LM), digital whole slide imaging (WSI), and artificial intelligence. The mitoses in this research were enumerated utilizing an artificial intelligence approach based on a 6-layer group CNN model. The findings of the paper showcased a high level of consistency between biopsies and resections regarding mitotic count methodologies. Both biopsies and resections exhibited substantial levels of agreement in BR across different modalities. The correlation coefficients (R2) between LM-MC and WSI-MC were 0.85 and 0.83, between LM-MC and AI-MC were 0.85 and 0.95, and between WSI-MC and AI-MC were 0.77 and 0.83.

This article [33] introduces an innovative approach to cancer cell profiling, utilizing Zernike image moments to extract intricate features from cancer cell images. The classification process is carried out using straightforward neural networks. Additionally, the research incorporates the Local Interpretable Model-Agnostic Explanations (LIME) technique and Explainable Artificial Intelligence (XAI) to provide insights into the test results. The methodology involves acquiring the BreakHis public dataset containing microscopic images and applying image processing and machine learning techniques in a high-throughput strategy. The proposed approach is theoretically supported and compared against contemporary methods, affirming its empirical foundation in algorithmic discovery. Notably, the system demonstrates an impressive ability to accurately differentiate between malignant and benign cancer cell images at a resolution of 40 $\times$ , achieving a commendable recognition rate of over 99%. Integrating XAI ensures that the machine learning model's results are interpretable and transparent, enhancing its reliability for subsequent analysis and parameter optimization.

### III. PROPOSED METHODOLOGY

This section discusses the image dataset and preprocessing techniques aimed at enhancing image quality. Additionally, it explores advanced transfer learning-based approaches for feature engineering and the classification of breast cancer grading.

The suggested methodology consists of several sections within the framework. Figure 1 provides a visual representation of the processes in the proposed framework. The initial phase encompasses image preprocessing and feature engineering. Multiple classical pre-trained models are constructed using image data. In the experimental phase, transfer learning approaches are employed for feature engineering and classification. The performance of each applied model is assessed. We introduce a novel transfer learning feature engineering mechanism that extracts features from preprocessed image data, contributing to enhanced performance in breast cancer diagnosis. Finally, we have

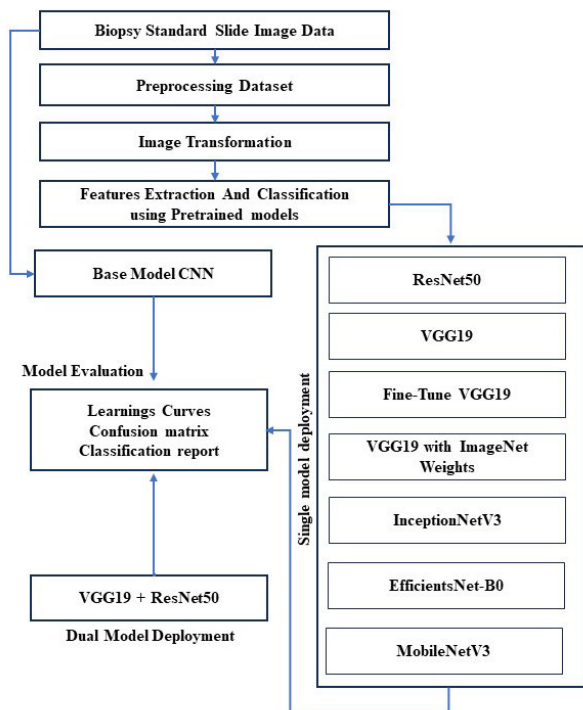


FIGURE 1. The workflow architecture of proposed study methodology.

developed a graphical user interface for a real-time application designed for breast cancer diagnosis.

**A. BREAST CELLS IMAGE DATASET**

The dataset image samples 906 were obtained from the Pour Sina Hakim Research Centre at Jimma University of Medical Sciences [34] in Iran. They consist of H&E-stained breast tissues collected from 124 patients identified between 2014 and 2019. The dataset is labeled with the name of the directory, witch contains images such as BC\_IDC\_Grade\_1, BC\_IDC\_Grade\_2, and BC\_IDC\_Grade\_3. Figure 14 illustrates the four distinct levels of magnification available: 4x, 10x, 20x, and 40x. In Figure 3, the dataset images undergo preprocessing using method along with visualization.

**B. IMAGE REPROCESSING AND TRANSFORMATION**

During image processing, we read image data using OpenCV and convert the image into RGB channels. The initial step involves converting the RGB channels into the HED color space [35], where HED represents Hue, Entropy, and Density. This color space is tailored for histopathology images, aiming to separate the image into three distinct channels effectively:

- Hue*: This channel represents the color of the tissue.
- Entropy*: This channel represents the amount of variation in the color of the tissue.
- Density*: This channel represents the amount of tissue in the image.

We performed stain normalization on the H and E channels individually. This involved adjusting the brightness and contrast of each channel to achieve greater uniformity. This

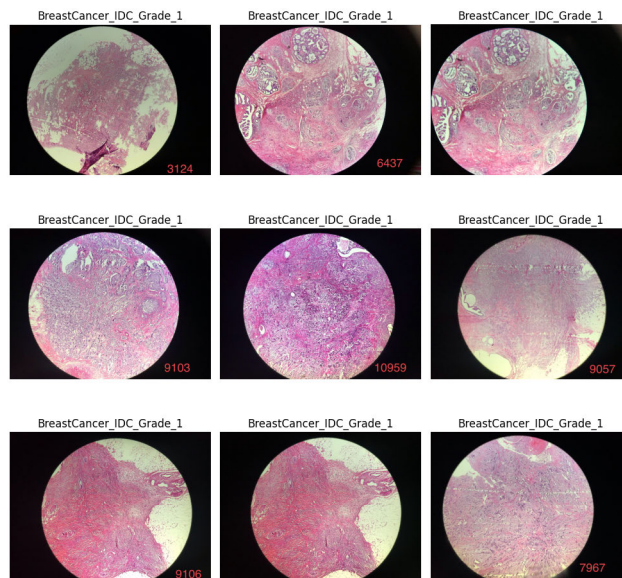


FIGURE 2. Without preprocessing histopathological images.

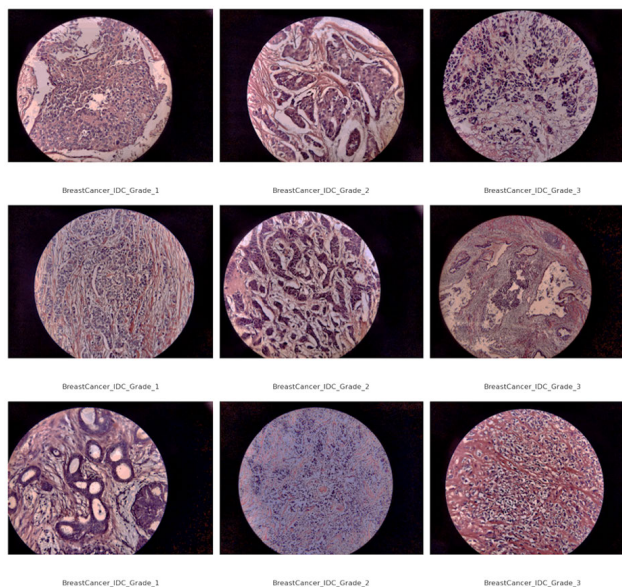


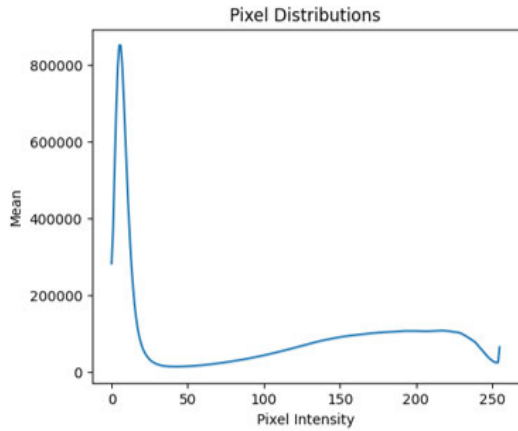
FIGURE 3. Preprocessed and normalized IDC breast cancer images.

step is crucial due to variations in staining intensities caused by different scanners and microscopes. The specific stain normalization method we utilized is known as CLAHE [36]. CLAHE is a technique that enhances image contrast by locally equalizing the histogram of each channel. This ensures that the brightness and contrast of each image region are harmonized, resulting in a more consistent distribution of pixel values within that region.

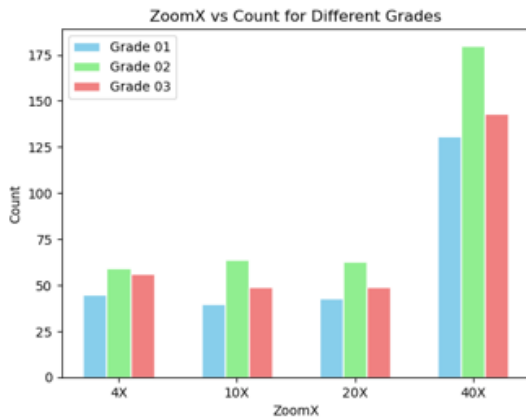
After the stain normalization process, we applied color augmentation to the image. This involved artificially altering the colors of the image to enhance diversity. This augmentation can prove beneficial in enhancing the performance of

**TABLE 2.** The properties analysis during the image preprocessing.

Property	Value
Hue channel mean	0.48
Hue channel standard deviation	0.17
Entropy channel mean	0.96
Entropy channel standard deviation	0.02
Density channel mean	0.72
Density channel standard deviation	0.05



(a)



(b)

**FIGURE 4.** The count plot analysis of dataset features.

machine learning models trained on histopathology images. As the final step in our preprocessing pipeline, we converted the image back to the RGB color space. This conversion marks the conclusion of our preprocessing procedures. The characteristics of the image post-preprocessing are detailed in Table 2.

Figure 4(a) displays the pixel distribution of the dataset images, while Figure 4(b) provides an overview of the relationship between grade, zoom level, and sample count for each cancer grade. Since the histopathological images are in the RGB color scheme, the pixel distributions of the dataset are plotted in Figures. Figure 5(a) displays Channel-1, Channel-2, and Channel-3, while Figure 5(b) illustrates the mean and standard deviation of each channel.

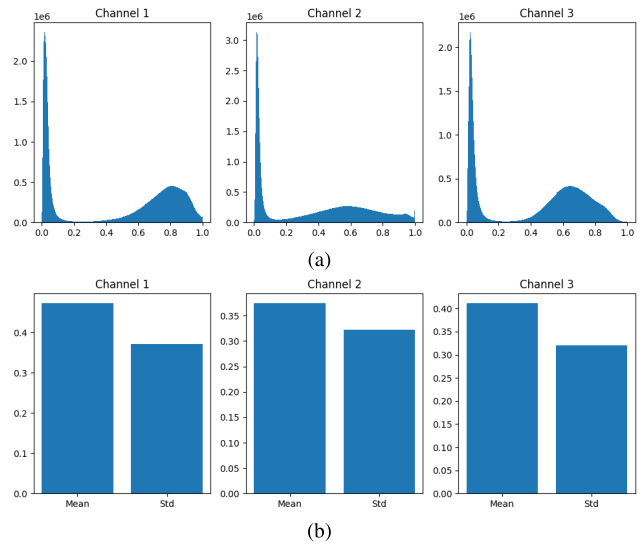


**FIGURE 5.** The pixel distributions are plot analysis.

**C. TRANSFER LEARNING**

We utilize transfer learning with multiple models [37], [38], [39]. We train and test the following models: VGG16, Fine-Tuned VGG16, VGG16 with ImageNet pre-training, ResNet50, InceptionNetV3, EfficientNet-B0, and MobileNetV3. Each model undergoes normalization through transformation after applying a staining filter, and the batch size is set to 16, with 10 epochs for each model.

ImageNet-trained CNNs learn generic characteristics [40]. These pre-trained programs recognize basic visual patterns and features to detect breast cancer. Transfer learning requires IDC breast cancer data, including labeled photographs of malignant and non-cancerous breast tissue. Training, validation, and testing datasets already exist [39]. Pre-trained CNN models extract features, with the network’s lower levels storing learned representations. The last convolutional or fully connected layer retrieves features from breast cancer images. These extracted features are then used to train a new classifier, which could be fully connected to neural networks using IDC dataset labels. The pre-trained model helps the classifier distinguish between cancerous and non-cancerous breast tissue.

Transfer learning enables the model to leverage extensive pre-trained model information and feature representations using limited IDC breast cancer data. This enhancement leads to improved accuracy and efficiency in diagnosing IDC breast cancer. The effectiveness of the model relies on the quality of the IDC breast cancer dataset.

**D. NOVEL TRANSFER FEATURES ENGINEERING**

In this research, we propose a novel transfer feature engineering technique aimed at enhancing performance in diagnosing breast cancer. The workflow architecture of our approach is illustrated in Figure 6. The proposed IVNet method extracts spatial features using layers inspired by the

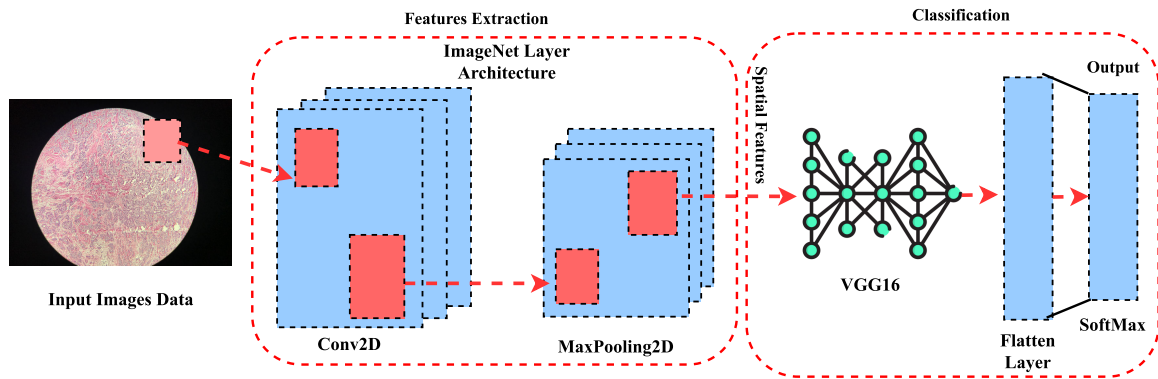


FIGURE 6. Our novel proposed feature engineering and diagnosis mechanism analysis.

ImageNet approach and applies them to the input dataset. These extracted features are then utilized for training and testing the VGG16 model. The integration of transfer learning features enables us to achieve high performance in breast cancer diagnosis.

#### E. PERFORMANCE EVALUATION

The performance of each applied classifier for breast cancer detection is assessed during model evaluations. Accuracy, precision, recall, and F1 score are employed to gauge the diagnostic performance of the model. Subsequently, the model is evaluated using the testing set and applied to breast cancer diagnosis. For the evaluation, an 80:20 ratio is utilized to split the image data into training and testing portions. The pre-trained model predicts breast cancer by analyzing breast images through the acquired classifier.

The performance metrics used for results evaluations are mathematically analyzed in this section. Accuracy gauges the overall correctness of predictions by measuring the ratio of correctly classified instances to the total. On the other hand, precision highlights the proportion of true positives among all positive predictions. Recall revealing the ratio of true positives to the sum of true and false negatives. The F1 score, which harmonizes precision and recall, is a balanced metric by computing the harmonic mean of the two. The following contains the mathematical working notations of metrics:

Accuracy:

$$\text{Accuracy} = \frac{\text{Number of Correct Predictions}}{\text{Total Number of Predictions}}$$

Precision:

$$\text{Precision} = \frac{\text{True Positives}}{\text{True Positives} + \text{False Positives}}$$

Recall:

$$\text{Recall} = \frac{\text{True Positives}}{\text{True Positives} + \text{False Negatives}}$$

F1 Score:

$$\text{F1 Score} = 2 \times \frac{\text{Precision} \times \text{Recall}}{\text{Precision} + \text{Recall}}$$

## IV. RESULTS AND DISCUSSIONS

In this section, we discuss the algorithms that have been deployed and present the results along with visualizations. Finally, we summarize these results to provide an overarching view of the overall performance of the model. According to the dataset, traditional machine learning methods do not contribute significantly to achieving the goal, whereas deep learning yields high classification scores.

### A. PERFORMANCE ANALYSIS WITH CLASSICAL APPROACHES

The performance of state-of-the-art classical approaches is evaluated through a series of metrics. The preprocessed image dataset is input into each pre-trained model for classification, and the results are assessed for comparative analysis.

#### 1) PERFORMANCE ANALYSIS OF CNN MODEL

We began by constructing a CNN model using the original image dataset and subsequently evaluated its performance. The performance analysis of the CNN model during training, based on time series data, is presented in Figure 7. The CNN model is executed for 10 epochs to assess performance outcomes. The analysis reveals that with increasing epochs, there is a decrease in loss and a gradual improvement in validation accuracy.

The classification report's analysis of the CNN model, utilizing unseen testing data, is comparatively evaluated in Figure 8. The analysis results indicate that, during diagnosis, the model achieves a low precision performance score of 0.54 for the diagnosis of Grade 2 breast cancer. However, it demonstrates a commendable recall score of 0.60 for the diagnosis of Grade 3 breast cancer. Overall, this analysis underscores that the CNN model has achieved subpar performance scores in these comparisons.

#### 2) PERFORMANCE ANALYSIS OF INCEPTIONNETV3 MODEL

After obtaining the initial performance scores, we implemented advanced image preprocessing techniques to enhance the performance. We utilized high-quality image data for



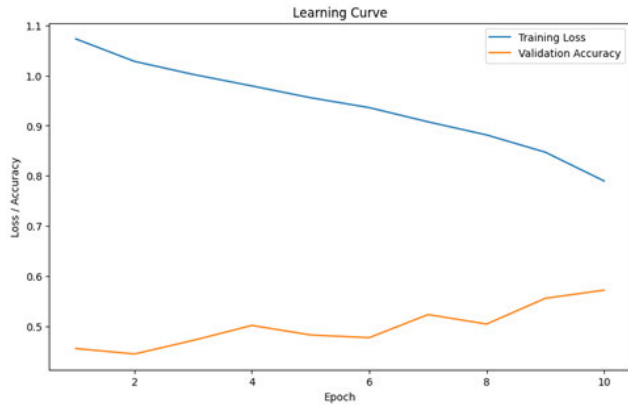


FIGURE 7. Time series-based performance analysis of CNN model during training.

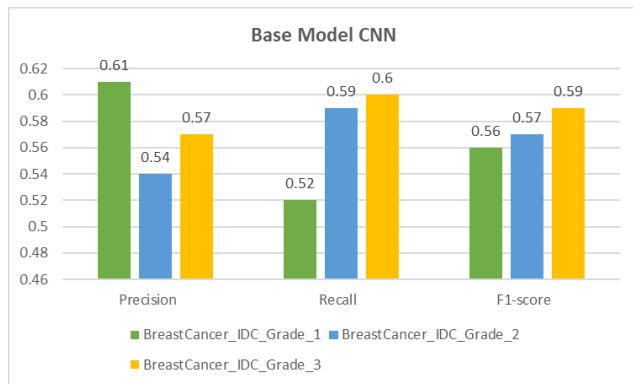


FIGURE 8. Classification report analysis of the CNN model using unseen testing data.

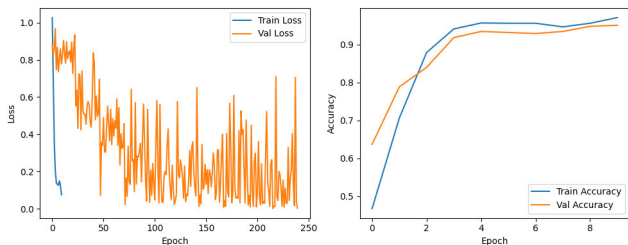


FIGURE 9. Time series-based performance analysis of INCEPTIONNETV3 model during training.

evaluating the results. The performance evaluation of the INCEPTIONNETV3 model during the training phase, utilizing time series data, is illustrated in Figure 9. The INCEPTIONNETV3 model underwent 10 epochs to assess its performance in diagnosing breast cancer. The analysis reveals a notable trend: as the number of epochs increased, there is a corresponding reduction in loss accompanied by a gradual improvement in validation accuracy. The performance metrics of the INCEPTIONNETV3 model exhibited strong results during training, consistently exceeding 0.90 in this analysis.

The analysis of the INCEPTIONNETV3 model in the classification report, using unseen testing data, is comparatively

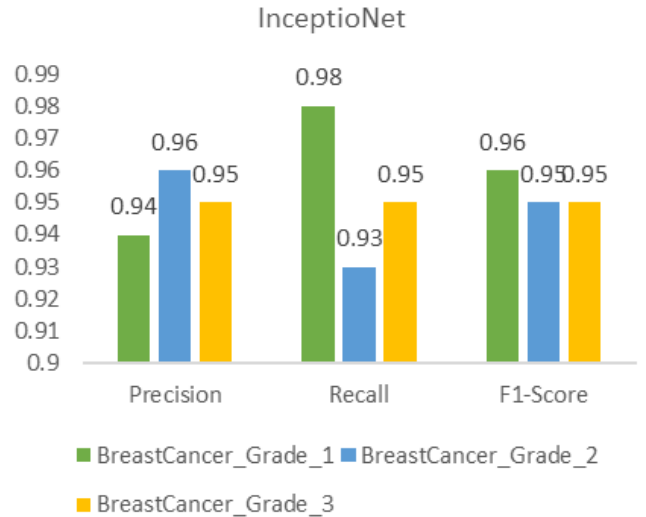


FIGURE 10. Classification report analysis of the INCEPTIONNETV3 model using unseen testing data.

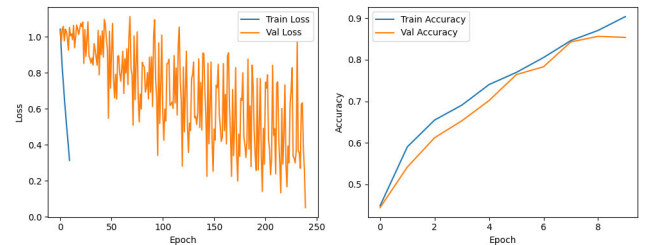


FIGURE 11. Time series-based performance analysis of EFFICIENTNET-B0 model during training.

evaluated in Figure 10. The results of the analysis indicate that the model performs well in diagnosing cases. It achieves a high recall score of 0.98 for grade 1 breast cancer diagnosis. The analysis demonstrates that the remaining performance scores are also good, ranging from 0.93 to 0.98. Overall, the performance scores of INCEPTIONNETV3 are commendable. However, there is still a need for further performance enhancement.

### 3) PERFORMANCE ANALYSIS OF EFFICIENTNET-B0 MODEL

The performance of another state-of-the-art approach, EFFICIENTNET-B0, is evaluated for comparisons. The performance evaluation of the EFFICIENTNET-B0 model during the training phase, utilizing time series data, is illustrated in Figure 11. The EFFICIENTNET-B0 model underwent 10 epochs to assess its performance in diagnosing breast cancer. The analysis shows that as the number of epochs increased, there is a corresponding reduction in loss, accompanied by a gradual improvement in validation accuracy. The performance metrics of the EFFICIENTNET-B0 model exhibited acceptable results during training, consistently below 0.90 in this analysis.

The analysis of the EFFICIENTNET-B0 model in the classification report, using unseen testing data, is comparatively

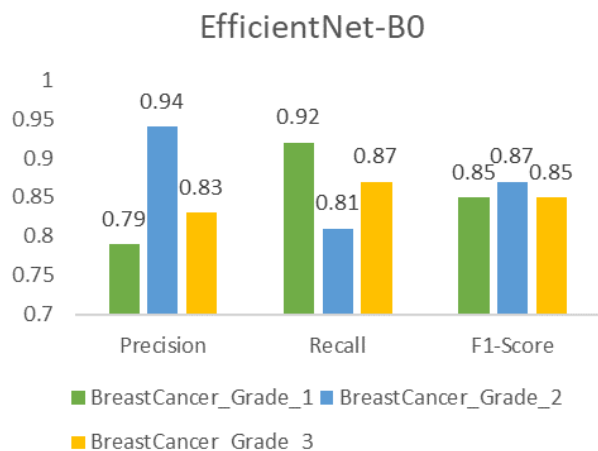


FIGURE 12. Classification report analysis of the EFFICIENTNET-B0 model using unseen testing data.

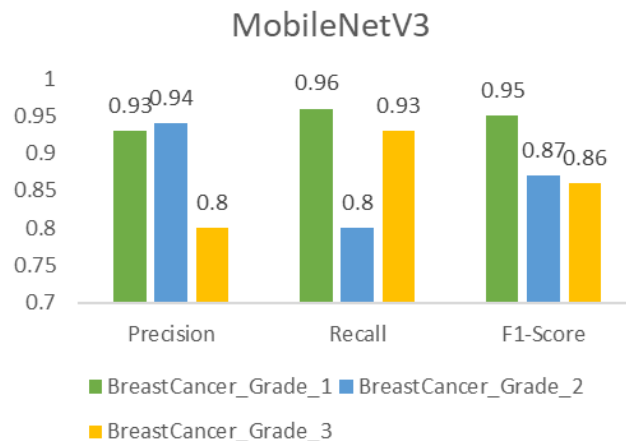


FIGURE 14. Classification report analysis of the MOBILENETV3 model using unseen testing data.

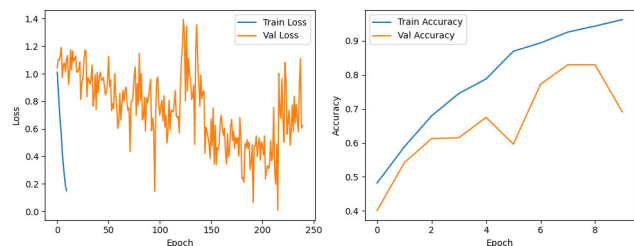


FIGURE 13. Time series-based performance analysis of MOBILENETV3 model during training.

evaluated in Figure 12. The results of the analysis indicate that the model performs well in diagnosing cases, achieving a high precision score of 0.94 for grade 2 breast cancer diagnosis. The analysis demonstrates that the remaining performance scores are also good, ranging from 0.79 to 0.94. However, while the overall performance scores of EFFICIENTNET-B0 are decent, they do not reach a high level. Therefore, further performance enhancements are still needed.

#### 4) PERFORMANCE ANALYSIS OF MOBILENETV3 MODEL

The performance of another state-of-the-art approach, MOBILENETV3, is evaluated for comparison. The performance evaluation of the MOBILENETV3 model during the training phase, utilizing time series data, is illustrated in Figure 13. The MOBILENETV3 model underwent 10 epochs to assess its performance in diagnosing breast cancer. The analysis shows that as the number of epochs increased, there is a corresponding reduction in loss, accompanied by a gradual improvement in validation accuracy. The analysis also demonstrated that validation accuracy decreased after epoch 6. The accuracy performance metrics of the MOBILENETV3 model exhibited acceptable results during training, consistently remaining below 0.90 in this analysis.

The analysis of the MOBILENETV3 model in the classification report, using unseen testing data, is comparatively evaluated in Figure 12. The results of the analysis indicate

that the model performs well in diagnosing cases, achieving a high recall score of 0.96 for grade 1 breast cancer diagnosis. The analysis demonstrates that the remaining performance scores are also good, ranging from 0.80 to 0.96. However, while the overall performance scores of MOBILENETV3 are decent, they do not reach a high level. Therefore, further enhancements in performance are still needed.

#### 5) PERFORMANCE ANALYSIS OF RESNET50 WITH IMAGENET MODEL

To evaluate the performance of the hybrid model [41], we combined RESNET50 with the ImageNet model and assessed the performance scores in this section. The performance evaluation of the RESNET50 with ImageNet model is conducted during the training phase using time series data, as depicted in Figure 15. The RESNET50 with ImageNet model is trained for 10 epochs to evaluate its effectiveness in diagnosing breast cancer. The analysis reveals that with an increasing number of epochs, there is a corresponding decrease in training loss, coupled with a gradual improvement in validation accuracy. However, the analysis also demonstrates that validation accuracy remains low throughout the training process. The accuracy performance metrics of the RESNET50 with ImageNet model exhibit suboptimal results during training, consistently staying below 0.70 in this analysis. Consequently, there is a clear need for performance enhancement techniques to achieve accurate diagnoses.

The analysis of the RESNET50 with ImageNet model in the classification report, using unseen testing data, is comparatively evaluated in Figure 16. The results of the analysis indicate that the model performs well in diagnosing cases, achieving a moderate recall score of 0.77 for grade 2 breast cancer diagnosis. The analysis demonstrates that the remaining performance scores are poor, ranging from 0.56 to 0.77. However, while the overall performance scores of RESNET50 with ImageNet are decent, they do not reach a high level. Therefore, further enhancements in performance are still needed.

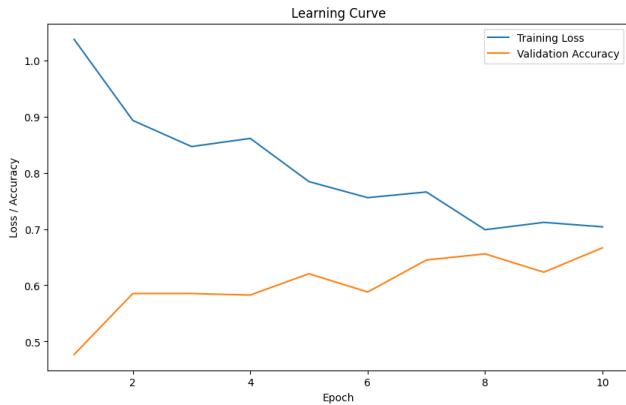


FIGURE 15. Time series-based performance analysis of RESNET50 with ImageNet model during training.

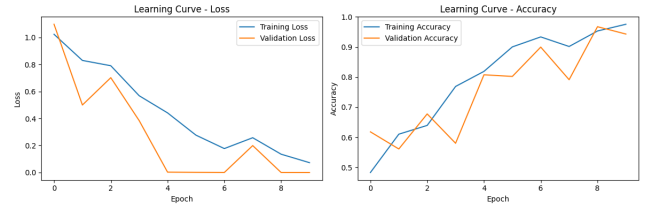


FIGURE 17. Time series-based performance analysis of proposed model during training.

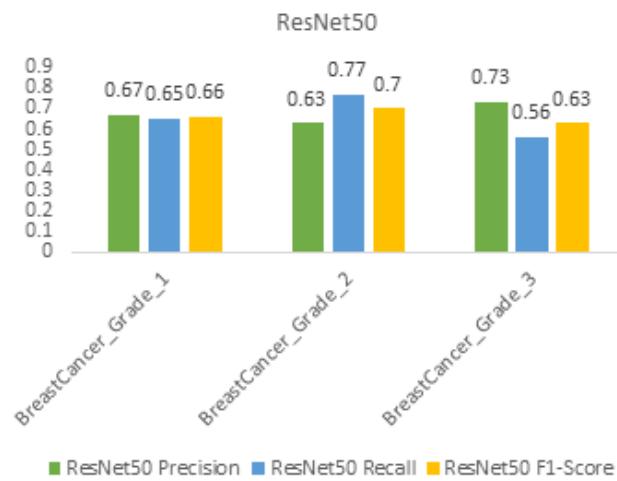


FIGURE 16. Classification report analysis of the RESNET50 with ImageNet model using unseen testing data.

**B. PERFORMANCE ANALYSIS WITH NOVEL PROPOSED APPROACH**

The performance evaluation of the proposed IVNet approach is presented in this section. The IVNet method extracts spatial features using layers inspired by the ImageNet approach and applies them to the input dataset. These extracted features are subsequently utilized for training and testing the VGG16 model. The results are then evaluated for performance validation.

To assess the performance of the proposed model, we combined VGG16 with the ImageNet architecture and evaluated its performance scores in this section. The evaluation of the proposed model’s performance took place during the training phase using time series data, as illustrated in Figure 17. The proposed model underwent 10 epochs of training to evaluate its effectiveness in diagnosing breast cancer. The analysis reveals that as the number of epochs increases, there is a corresponding decrease in training loss, accompanied by a gradual improvement in validation accuracy. Furthermore,

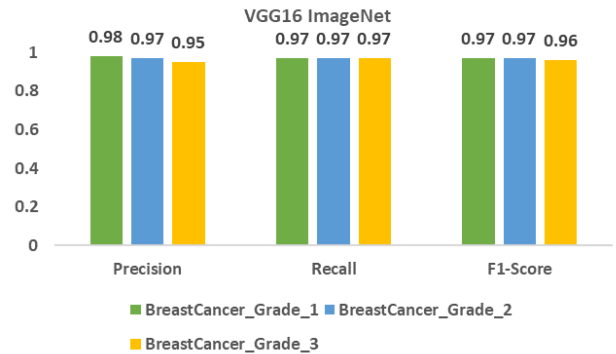


FIGURE 18. Classification report analysis of the proposed model using unseen testing data.

this analysis demonstrates that the validation accuracy consistently reached its maximum throughout the training process. The accuracy performance metrics of the proposed model showcased the best results during training, consistently remaining within the range of 99% to 100% in this analysis, which is best compared to others.

The performance of the proposed model is analyzed in the classification report using unseen testing data, as shown in Figure 18. The results of the analysis indicate that the model excels in diagnosing cases, achieving a precision score of 0.98 for grade 1 breast cancer diagnosis, which is the highest. Furthermore, the analysis demonstrates consistently strong performance across the board, with scores ranging from 0.95 to 0.98. In conclusion, this analysis supports the claim that our proposed model outperforms the state-of-the-art approach, displaying high efficacy when applied to unseen testing data.

The confusion matrix analysis, based on performance evaluation for each target class, is conducted as illustrated in Figure 19. The analysis shows that the proposed approach achieved a minimal error rate in wrong predictions during the diagnosis of breast cancer from unseen testing data. This analysis validates the high-performance scores of the proposed approach, with a high rate of correct predictions for the diagnosis of breast cancer.

In conclusion, this analysis highlights that our innovative approach achieved high performance scores during training, surpassing the performance of other state-of-the-art approaches that were applied.

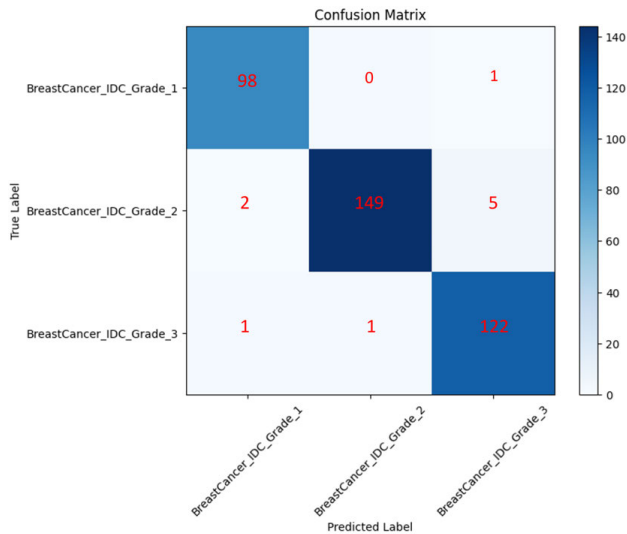


FIGURE 19. Confusion matrix analysis of the proposed approach.

TABLE 3. The comparative performance analysis of applied models.

Models	Precision	Recall	F1	Accuracy
CNN Base Model	0.75	0.74	0.75	0.75
ImageNet + ResNet50	0.68	0.66	0.66	0.67
VGG16	0.74	0.57	0.57	0.59
Fine Tune VGG16	0.67	0.64	0.64	0.64
InceptionNetV3	0.95	0.95	0.95	0.95
EfficientNet-B0	0.85	0.86	0.86	0.86
MobileNetV3	0.89	0.90	0.89	0.89
<b>ImageNet + VGG16 (IVNet)</b>	<b>0.97</b>	<b>0.97</b>	<b>0.97</b>	<b>0.97</b>

### 1) PERFORMANCE COMPARISON OF THE PROPOSED APPROACH WITH OTHERS

The overall performance of our proposed approach is compared with the current state-of-the-art method, as presented in Table 3. The analysis reveals that our CNN Model achieves an F1 score of 0.75, a recall of 0.74, and a precision of 0.75, resulting in an overall accuracy of 0.75. In contrast, the ResNet50 + ImageNet model attains an accuracy of 0.67, accompanied by relatively lower precision, recall, and F1-score values. The VGG16 model consistently demonstrates scores of 0.74 for F1-score, precision, and recall, although the recall rate is notably lower at 0.57. The Fine-Tuned VGG16 model exhibits uniform values of 0.67 for precision, recall, and F1-score, while accuracy and precision are both recorded at 0.64. This analysis underscores exceptional performance across various metrics.

The proposed VGG16 With ImageNet model achieves a remarkable accuracy of 0.97, accompanied by the corresponding precision, recall, and F1-score values also at 0.97. The InceptionNetV3 model also achieves a notable accuracy of 0.95, owing to its robust precision, recall, and F1 score. Additionally, the EfficientNet-B0 model attains an accuracy of 0.86, surpassing other models in the lineup. This comprehensive comparative analysis demonstrates that our

TABLE 4. Comparisons of the proposed approach using benchmark state-of-the-art datasets.

State of the art Data	Precision	Recall	F1-Score	Accuracy
Previous study data 1	0.89	0.89	0.89	0.90
Previous study data 2	0.89	0.89	0.89	0.90
<b>Our dataset</b>	<b>0.97</b>	<b>0.97</b>	<b>0.97</b>	<b>0.97</b>

TABLE 5. The statistical t-test analysis of proposed approach against applied methods.

Case	Statistics Score	P value	Null hypothesis
Proposed IVNet vs. CNN Model	-89.0	1.3555	Rejected
Proposed IVNet vs. VGG16 Model	-8.57	0.0001	Rejected
Proposed IVNet vs. ImageNet + ResNet50 Model	-63.1	1.0560	Rejected
Proposed IVNet vs. InceptionNetV3 Model	-inf	0.0000	Rejected
Proposed IVNet vs. EfficientNet-B0 Model	-45.0	8.0659	Rejected
Proposed IVNet vs. MobileNetV3 Model	-31.0	7.4823	Rejected

proposed approach outperforms the state-of-the-art method, exhibiting high-performance scores for diagnostic tasks.

### C. COMPARISON USING OTHER STATE OF THE ART STUDIES DATA

The performance of our proposed approach is validated using a benchmark dataset used in this study [42]. The performance comparisons show that our proposed approach also achieved high-performance scores of 90% for a benchmark dataset. The performance results are analyzed in Table 4.

### D. STATISTICAL T-TEST ANALYSIS

In this section, we present the results of a statistical t-test analysis to evaluate the effectiveness of our proposed model. This test demonstrates the importance of our approach by examining two hypotheses. The null hypothesis suggests that our method lacks statistical significance compared to others. If the t-test rejected this hypothesis, it would indicate support for the alternative hypothesis, confirming the statistical significance of our proposed approach. The t-test generates a Statistic Score and an associated p-value. If the p-value exceeds the Statistic value, it leads to rejecting the null hypothesis. The outcomes are detailed in Table 5 for various scenarios. We compared the results of our proposed deep learning model using the recommended methodology against other applied models. In every comparison, the t-test rejects the null hypothesis, offering proof of the statistical significance of our proposed approach.

### E. REALTIME DIAGNOSIS WITH GUI-BASED APPLICATION

In this study, for the real-time diagnosis of breast cancer, we have developed a GUI-based application, as depicted in Figure 21. Our proposed IVNet approach has been implemented in the backend of this application. Medical specialists

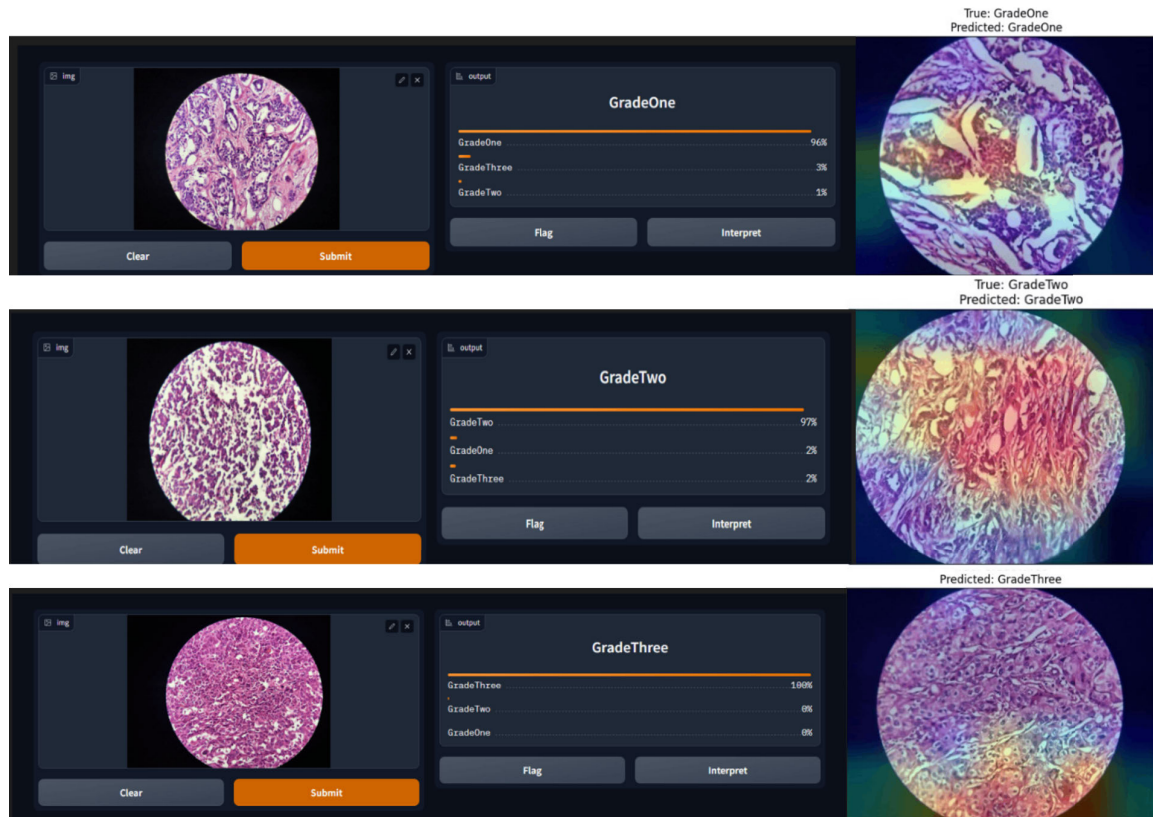


FIGURE 20. The real-time diagnosis of breast cancer using a GUI application.

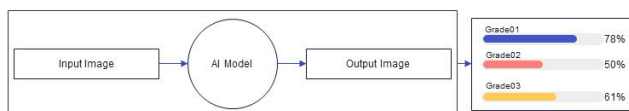


FIGURE 21. The backend functionality of real-time diagnosis of breast cancer using a GUI application.

can simply upload an image within the application, enabling it to diagnose cancer and predict its stages efficiently. This application expedites the diagnosis process, yielding high-performance accuracy scores.

## V. CONCLUSION

This research proposes a novel approach to breast cancer grading mechanisms based on histopathology images. The proposed transfer learning approach aims to enhance performance in diagnosing breast cancer. The IVNet method, as part of this approach, extracts spatial features using layers inspired by the ImageNet approach and applies them to the input dataset. These extracted features are then utilized for training and testing the VGG16 model to categorize breast cancer images into Grade 01, Grade 02, and Grade 03. The study's findings demonstrate that the proposed method is highly accurate and sensitive when applied to grading breast cancer. The GUI-based application has the potential to

contribute valuable data to treatment planning and prognosis, underscored by its positive performance. Pathologists and clinicians can adopt this technique as a decision support system, particularly beneficial in low-resource settings where specialists and necessary tools might be scarce. The proposed method offers a faster and more objective alternative to the time-consuming and subjective manual grading process in histopathology.

## REFERENCES

- [1] A. R. Anik, K. Hasan, M. M. Islam, M. M. Hasan, M. F. Ali, and S. K. Das, "Non-invasive portable technologies for monitoring breast cancer related lymphedema to facilitate telehealth: A scoping review," *IEEE J. Biomed. Health Informat.*, vol. 27, no. 9, pp. 4524–4535, Sep. 2023.
- [2] L. Liu, Y. Wang, P. Zhang, H. Qiao, T. Sun, H. Zhang, X. Xu, and H. Shang, "Collaborative transfer network for multi-classification of breast cancer histopathological images," *IEEE J. Biomed. Health Informat.*, early access, Jun. 9, 2023, doi: [10.1109/JBHI.2023.3283042](https://doi.org/10.1109/JBHI.2023.3283042).
- [3] Y. Jun, S. Jin, N. Myung, J. Jeong, J. Lee, and H. J. Cho, "TS-Net: A deep learning framework for automated assessment of longitudinal tumor volume changes in an orthotopic breast cancer model using MRI," *IEEE Access*, vol. 11, pp. 55117–55125, 2023.
- [4] S. Ferrari, E. Tagliabue, B. M. Maris, and P. Fiorini, "Autonomous robotic system for breast biopsy with deformation compensation," *IEEE Robot. Autom. Lett.*, vol. 8, no. 3, pp. 1215–1222, Mar. 2023.
- [5] A. M. Qadri, A. Raza, F. Eid, and L. Abualigah, "A novel transfer learning-based model for diagnosing malaria from parasitized and uninfected red blood cell images," *Decis. Anal. J.*, Nov. 2023, Art. no. 100352.

- [6] S. Jácobo-Zavaleta and J. Zavaleta, "Needle placement for robot-assisted 3D-guided ultrasound breast biopsy: A preliminary study," *IEEE Latin Amer. Trans.*, vol. 21, no. 3, pp. 450–456, Mar. 2023.
- [7] S. Goudarzi, J. Whyte, M. Boily, A. Towers, R. D. Kilgour, and H. Rivaz, "Segmentation of arm ultrasound images in breast cancer-related lymphedema: A database and deep learning algorithm," *IEEE Trans. Biomed. Eng.*, vol. 70, no. 9, pp. 2552–2563, Mar. 2023.
- [8] X. Zhou and X. Yin, "Faster boundary-aware transformer for breast cancer segmentation," in *Proc. 15th Int. Conf. Adv. Comput. Intell. (ICACI)*, May 2023, pp. 1–6.
- [9] F. Anique, R. Liu, M. U. Farooq, S. S. Oh, J. K. Jo, and S. Y. Ko, "Multiple tissue sample collection device for MRI guided transrectal prostate biopsy: Optimization and MRI compatibility tests," *IEEE Access*, vol. 11, pp. 76486–76497, 2023.
- [10] C. Ciminelli, P. Colapietro, G. Brunetti, and M. N. Armenise, "Lab-on-chip for liquid biopsy: A new approach for the detection of biochemical targets," in *Proc. 23rd Int. Conf. Transparent Opt. Netw. (ICTON)*, Jul. 2023, pp. 1–4.
- [11] C. Ganesh, T. Jeevitha, A. Jayalakshmi, M. Shanthini, N. S. Kumar, and P. Malini, "A survey of breast cancer detection using medical imaging techniques," in *Proc. 9th Int. Conf. Adv. Comput. Commun. Syst. (ICACCS)*, vol. 1, Mar. 2023, pp. 873–876.
- [12] W. M. Shaban, A. A. Abdullah, and E. Ashraf, "An in-depth review of AI-based techniques for early diagnosis of breast cancer: Evaluation of CAD system design and classification methodologies," in *Proc. Int. Telecommun. Conf. (ITC-Egypt)*, Jul. 2023, pp. 322–329.
- [13] S. Díaz-Santos and D. Escanez-Exposito, "Classical vs. Quantum machine learning for breast cancer detection," in *Proc. 19th Int. Conf. Design Reliable Commun. Netw. (DRCN)*, Apr. 2023, pp. 1–5.
- [14] V. L. K. Vasista, K. Sona, J. Pedarla, B. Sahithi, T. K. R. K. Rao, and K. B. Prakash, "Predicting breast cancer using classical machine learning and deep learning algorithms," in *Proc. Int. Conf. Intell. Innov. Technol. Comput., Electr. Electron. (IITCEE)*, Jan. 2023, pp. 988–991.
- [15] H. S. Park, Y. Chong, Y. Lee, K. Yim, K. J. Seo, G. Hwang, D. Kim, G. Gong, N. H. Cho, C. W. Yoo, and H. J. Choi, "Deep learning-based computational cytopathologic diagnosis of metastatic breast carcinoma in pleural fluid," *Cells*, vol. 12, no. 14, p. 1847, Jul. 2023.
- [16] S. Çayır, B. Darbaz, G. Solmaz, Ç. Yazıcı, H. Kusetogullari, F. Tokat, L. O. Ithem, E. Bozaba, E. Tekin, and G. Özsoy, "Patch-based approaches to whole slide histologic grading of breast cancer using convolutional neural networks," in *Diagnostic Biomedical Signal and Image Processing Applications with Deep Learning Methods*. Amsterdam, The Netherlands: Elsevier, 2023, pp. 103–118.
- [17] A. Raza, H. U. R. Siddiqui, K. Munir, M. Almutairi, F. Rustam, and I. Ashraf, "Ensemble learning-based feature engineering to analyze maternal health during pregnancy and health risk prediction," *PLoS ONE*, vol. 17, no. 11, Nov. 2022, Art. no. e0276525.
- [18] Y. Liu, D. Han, A. V. Parwani, and Z. Li, "Applications of artificial intelligence in breast pathology," *Arch. Pathol. Lab. Med.*, vol. 147, no. 9, pp. 1003–1013, Sep. 2023.
- [19] M. López-Pérez, P. Morales-Álvarez, L. A. D. Cooper, R. Molina, and A. K. Katsaggelos, "Deep Gaussian processes for classification with multiple noisy Annotators. Application to breast cancer tissue classification," *IEEE Access*, vol. 11, pp. 6922–6934, 2023.
- [20] A. Rehman, A. Raza, F. S. Alamri, B. Alghofaily, and T. Saba, "Transfer learning-based smart features engineering for osteoarthritis diagnosis from knee X-ray images," *IEEE Access*, vol. 11, pp. 71326–71338, 2023.
- [21] Y. Wang, B. Acs, S. Robertson, B. Liu, L. Solorzano, C. Wahlby, J. Hartman, and M. Rantalainen, "Improved breast cancer histological grading using deep learning," *Ann. Oncol.*, vol. 33, no. 1, pp. 89–98, Jan. 2022.
- [22] A. Raza, A. M. Qadri, I. Akhtar, N. A. Samee, and M. Alabdulhafith, "LogRF: An approach to human pose estimation using skeleton landmarks for physiotherapy fitness exercise correction," *IEEE Access*, vol. 11, pp. 107930–107939, 2023.
- [23] R. Jaroensri, "Deep learning models for histologic grading of breast cancer and association with disease prognosis," *NPJ Breast Cancer*, vol. 8, no. 1, p. 113, Oct. 2022.
- [24] S. C. Wetstein, V. M. T. de Jong, N. Stathonikos, M. Opdam, G. M. H. E. Dackus, J. P. W. Pluim, P. J. van Diest, and M. Veta, "Deep learning-based breast cancer grading and survival analysis on whole-slide histopathology images," *Sci. Rep.*, vol. 12, no. 1, Sep. 2022, Art. no. 15102.
- [25] I. O. Ellis, E. A. Rakha, G. M. Tse, and P. H. Tan, "An international unified approach to reporting and grading invasive breast cancer. An overview of the international collaboration on cancer reporting (ICCR) initiative," *Histopathology*, vol. 82, no. 1, pp. 189–197, Jan. 2023.
- [26] R. Yan, F. Ren, J. Li, X. Rao, Z. Lv, C. Zheng, and F. Zhang, "Nuclei-guided network for breast cancer grading in HE-stained pathological images," *Sensors*, vol. 22, no. 11, p. 4061, May 2022.
- [27] S. Mantrala, P. S. Ginter, A. Mitkari, S. Joshi, H. Prabhala, V. Ramachandra, L. Kini, R. Idress, T. M. D'Alfonso, S. Fineberg, S. Jaffer, A. K. Sattar, A. B. Chagpar, P. Wilson, K. Singh, M. Harigopal, and D. Koka, "Concordance in breast cancer grading by artificial intelligence on whole slide images compares with a multi-institutional cohort of breast pathologists," *Arch. Pathol. Lab. Med.*, vol. 146, no. 11, pp. 1369–1377, Nov. 2022.
- [28] A. Ibrahim, M. S. Toss, S. Makhlof, I. M. Miligy, F. Minhas, and E. A. Rakha, "Improving mitotic cell counting accuracy and efficiency using phosphohistone-H3 (PHH3) antibody counterstaining with haematoxylin and eosin as part of breast cancer grading," *Histopathology*, vol. 82, no. 3, pp. 393–406, Feb. 2023.
- [29] M. M. Köteles, A. Vigdorovits, D. Kumar, I.-M. Mihai, A. Jurescu, A. Gheju, A. Bucur, O. O. Harich, and G.-E. Olteanu, "Comparative evaluation of breast ductal carcinoma grading: A deep-learning model and general Pathologists' assessment approach," *Diagnostics*, vol. 13, no. 14, p. 2326, Jul. 2023.
- [30] S. A. van Bergeijk, N. Stathonikos, N. D. ter Hoeve, M. W. Lafarge, T. Q. Nguyen, P. J. van Diest, and M. Veta, "Deep learning supported mitoses counting on whole slide images: A pilot study for validating breast cancer grading in the clinical workflow," *J. Pathol. Informat.*, vol. 14, Jan. 2023, Art. no. 100316.
- [31] A. Raza, K. Munir, and M. Almutairi, "A novel deep learning approach for deepfake image detection," *Appl. Sci.*, vol. 12, no. 19, p. 9820, Sep. 2022.
- [32] F. Rustam, A. Raza, I. Ashraf, and A. D. Jurcut, "Deep ensemble-based efficient framework for network attack detection," in *Proc. 21st Medit. Commun. Comput. Netw. Conf. (MedComNet)*, Jun. 2023, pp. 1–10.
- [33] D. Kaplun, A. Krasichkov, P. Chetyrbok, N. Oleinikov, A. Garg, and H. S. Pannu, "Cancer cell profiling using image moments and neural networks with model agnostic explainability: A case study of breast cancer histopathological (BreakHis) database," *Mathematics*, vol. 9, no. 20, p. 2616, Oct. 2021.
- [34] H. Bolhasani. (2021). *Breast Cancer Grading* | Kaggle. Accessed: Aug. 17, 2023. [Online]. Available: <https://www.kaggle.com/datasets/bolhasani/breast-cancer-grading>
- [35] M. F. Nahl, I. A. Dewi, and K. R. Putra, "Holistically-nested edge detection in chair ergonomic detection," *AIP Conf. Proc.*, vol. 2772, no. 1, 2023, Art. no. 080013.
- [36] M. Mehdizadeh, K. T. Tafti, and P. Soltani, "Evaluation of histogram equalization and contrast limited adaptive histogram equalization effect on image quality and fractal dimensions of digital periapical radiographs," *Oral Radiol.*, vol. 39, no. 2, pp. 418–424, Apr. 2023.
- [37] P. Marcelino, "Transfer learning from pre-trained models," *Towards Data Sci.*, vol. 10, p. 23, Oct. 2018.
- [38] A. Raza, F. Rustam, B. Mallampati, P. Gali, and I. Ashraf, "Preventing crimes through gunshots recognition using novel feature engineering and meta-learning approach," *IEEE Access*, vol. 11, pp. 103115–103131, 2023.
- [39] A. Raza, K. Munir, M. S. Almutairi, and R. Sehar, "Novel class probability features for optimizing network attack detection with machine learning," *IEEE Access*, vol. 11, pp. 98685–98694, 2023.
- [40] R. Mahadeva, S. P. Patole, V. Patel, V. Chaurasia, A. Sharma, and R. Sharma, "Deep transfer learning with multi-level features extraction approach for breast cancer classification," in *Proc. 1st Int. Conf. Innov. High Speed Commun. Signal Process. (IHCSPP)*, Mar. 2023, pp. 471–474.
- [41] A. Raza, F. Rustam, H. U. R. Siddiqui, I. D. L. T. Diez, and I. Ashraf, "Predicting microbe organisms using data of living micro forms of life and hybrid microbes classifier," *PLoS ONE*, vol. 18, no. 4, Apr. 2023, Art. no. e0284522.
- [42] K. A. Elsharawy, T. A. Gerds, E. A. Rakha, and L. W. Dalton, "Artificial intelligence grading of breast cancer: A promising method to refine prognostic classification for management precision," *Histopathology*, vol. 79, no. 2, pp. 187–199, Aug. 2021.

**SAMEEN AZIZ** is currently pursuing the Ph.D. degree in information technology with the Khwaja Fareed University of Engineering and Information Technology (KFUEIT). She is a Research Assistant with the Fareed Computing and Research Center, KFUEIT. Her current research interests include data mining, mainly working machine learning, decision trees, deep learning, artificial intelligence, and image processing.



**KASHIF MUNIR** received the B.Sc. degree in mathematics and physics from Islamia University Bahawalpur, Pakistan, in 1999, the M.Sc. degree in information technology from University Sains Malaysia, in 2001, the M.S. degree in software engineering from the University of Malaya, Malaysia, in 2005, and the Ph.D. degree in informatics from the Malaysia University of Science and Technology, Malaysia, in 2015. He has been in the field of higher education, since 2002. After an initial teaching experience with courses with the Binary College, Malaysia, for one semester, and the Stamford College, Malaysia, for around four years. Later, he relocated to Saudi Arabia. He was with the King Fahd University of Petroleum and Minerals, Saudi Arabia, from September 2006 to December 2014. He was with the University of Hafr Al-Batin, Saudi Arabia, in January 2015. In July 2021, he joined the Khwaja Farid University of Engineering and IT, Rahim Yar Khan. He is currently an Assistant Professor with the IT Department. He has published journal articles, conference papers, books, and book chapters. His current research interests include cloud computing security, software engineering, and project management. He has been with the technical program committee of many peer-reviewed conferences and journals, where he reviewed many research articles.



**ALI RAZA** received the B.Sc. and M.Sc. degrees in computer science from the Department of Computer Science, Khwaja Fareed University of Engineering and Information Technology (KFUEIT), Rahim Yar Khan, Pakistan, in 2021. He has published several articles in reputed journals. His current research interests include data science, artificial intelligence, data mining, natural language processing, machine learning, deep learning, and image processing.



**MUBARAK S. ALMUTAIRI** received the B.Sc. degree in systems engineering from the King Fahd University of Petroleum and Minerals, Dhahran, Saudi Arabia, in 1997, the M.Sc. degree in industrial and systems engineering from the University of Florida, Gainesville, FL, USA, in 2003, and the Ph.D. degree in systems design engineering from the University of Waterloo, Waterloo, Canada, in 2007. From 1997 to 2000, he was an Industrial Engineer with the Saudi Arabia Oil Company (Aramco). He is currently an Associate Professor with the Computer Science and Engineering Department, University of Hafr Albatin, Hafr Albatin, Saudi Arabia. His current research interests include decision analysis, expert systems, risk assessment, information security, fuzzy logic, and mobile government applications.



**SHOAB NAWAZ** received the M.S.C.S. degree from the University of South Asia, Lahore. He is a Data Science Freelancer. His current research interests include data mining, mainly working on AI and deep learning-based text mining, and data science management technologies. He has expertise as an IT Engineer/System Support Engineer in the sales and distributions, financial services, health care, and logistics fields. Strong management skills, able to interface with all levels of technical and business resources. Managing resources, such as servers, assets, ERP applications, websites, and network devices, resolving users' complaints, on-premises and cloud-based resiliency and recoverability validation, security firewall, ACL, and database. Extensive experience with technical analysis of third-party vendors and testing validation. He received the Azure Cloud Certified Professional for the master's degree.

...